Coccolithophore responses to environmental variability in the South China Sea: species composition and calcite content

X.B. Jin[1], C.L. Liu[1], A.J. Poulton[2], M.H. Dai[3] and X.H. Guo[3]

[1]State Key Laboratory of Marine Geology, Tongji University, Shanghai 200092, China
[2]Ocean Biogeochemistry and Ecosystems, National Oceanography Centre, Southampton, UK
[3]State Key Laboratory of Marine Environmental Science, Xiamen University, Xiamen 361005, China

Correspondence to: C.L. Liu (liucl@tongji.edu.cn)

Abstract. Coccolithophore contributions to the global marine carbon cycle are regulated by the calcite content of their scales (coccoliths), and the relative cellular levels of photosynthesis and calcification rates. All three of these factors vary between coccolithophore species, and with response to the growth environment. Here, water samples were collected in the northern basin of the South China Sea (SCS) during summer 2014 in order to examine how environmental variability influenced species composition and cellular levels of calcite content. Average coccolithophore abundance and their calcite concentration in the water-column were 11.82 cells ml^{-1} and 1508.3 pg C ml^{-1}, respectively during the cruise. Water samples can be divided into 3 floral groups according to their distinct coccolithophore communities. The vertical structure of the coccolithophore community in the water-column was strongly regulated by mesoscale eddies across the SCS basin. The evaluation of coccolithophore-based calcite in the surface-ocean also showed that three key species in the SCS (*Emiliania huxleyi*, *Gephyrocapsa oceanica*, *Florisphaera profunda*) and other larger, numerically rare species made almost equal contributions to total coccolith-based calcite in the water column. For *Emiliania huxleyi* biometry measurements, coccolith size positively correlated with nutrients (nitrate, phosphate), and it is suggested that coccolith distal length is influenced by light and nutrients through regulation of growth rates. Larger sized coccoliths were also linked statistically to low pH and calcite saturation states, however it is not a simple cause and effect relationship, as carbonate chemistry was strongly co-correlated with the other key environmental factors (nutrients, light).

1 Introduction

Coccolithophores are an important component of marine plankton communities, contributing globally to both the organic carbon pump (biological carbon pump) and the (calcium) carbonate (counter) pump. Coccolithophores may contribute 10% to 20% of total chlorophyll-*a*, primary production and 30% to 60% of calcium carbonate (calcite or particulate inorganic carbon) in the water-column in non-bloom conditions (Poulton et al., 2006, 2007, 2010, 2014), although higher contributions of organic carbon (>40%) do occur in coccolithophore blooms (Poulton et al., 2013). Coccolith-based calcite can contribute up to 80% to deep-sea carbonate fluxes (Sprengel et al., 2000, 2002; Young and Ziveri, 2000). High concentrations of the cosmopolitan coccolithophore species *Emiliania huxleyi* can generate large quantities of cells and detached coccoliths (e.g. ~2000 cells ml^{-1} and 3×10^5 coccoliths ml^{-1}, Balch et al., 1991), which are detectable from space (Cokacar et al., 2004; Raitsos et al., 2006); for example, the "Great Calcite Belt" in the Southern Hemisphere is attributed to high particulate inorganic carbon from coccolithophores (Balch et al., 2011, 2014). To assess the contribution of coccolithophores to the carbon cycle, two relevant issues are worthy of attention: (1) coccolithophore species composition and calcite concentration in the water-column, and (2) their calcification response to oceanic environmental factors.

The SCS is the largest marginal sea in the west Pacific Ocean, covering an area of 3.5×10^6 km^2 (Wang et al., 2014). Phytoplankton production and surface circulation in the northern basin of the SCS are greatly influenced by the East Asian monsoon system. In the northern part of SCS, during the summer season (June to August), the surface water is oligotrophic and well stratified, and a stable mixed layer is developed. The mean chlorophyll-*a* concentration and primary production in

the euphotic zone is 0.08 ± 0.03 mg m^{-3} and <30 mg C m^{-2} d^{-1}, respectively (Chen, 2005; Chen et al., 2006), with the nitricline at a depth of ~60 m (Chen et al., 2006). During the winter season (December to February), surface waters are productive and well mixed due to the strong seasonal wind stress. Mean chlorophyll-*a* concentrations and primary production are 0.65 ± 0.17 mg m^{-3} and 550 mg C m^{-2} d^{-1}, respectively (Chen, 2005; Chen et al., 2006), with the nitricline much shallower at around 5 m to 20 m (Chen et al., 2006). Some preliminary work on coccolithophore biogeography have been reported in the SCS (Okada and Honjo, 1975; Chen et al., 2007a; Sun et al., 2011), however these studies are confined to surface waters or sporadic sampling sites and lack any coccolith weight estimation.

Mesoscale eddies are typical physical oceanographic features in the SCS (Wang et al., 2003), and significantly influence the structure of the upper water-column. Cyclonic eddies in the SCS cause the thermocline to shallow and thin, while anti-cyclonic eddies have the opposite effect (Chen et al., 2011). Eddy activity in the SCS are related to local wind stress curl, intrusion of the Kuroshio Current and coastal baroclinic jets (Wang et al., 2003; Hu et al., 2011). Cold-water cyclonic eddies can elevate the nutricline into subsurface waters and drive enhanced phytoplankton production at levels exceeding those in the winter. For example, the average integrated primary production inside eddies in spring and in winter is 1090 and 550 mg C m^{-2} d^{-1}, respectively (Chen, 2005; Chen et al., 2007b). Modeling studies have reported that cyclonic eddies are significant nutrient sources fueling the biological carbon pump in the SCS (Xiu and Chai, 2011). Pigments determined by high-performance liquid chromatography have also shown that phytoplankton assemblages relate to mesoscale eddies in the SCS (Huang et al., 2010; Wang et al., 2016), however how coccolithophore communities respond to these regular oceanographic phenomena is still unclear.

Decreasing ocean pH (termed ocean acidification), in response to increasing atmospheric and seawater CO_2 levels, is a major concern for marine calcifiers such as coccolithophores, as lower pH levels (and calcium carbonate saturation levels, Ω_C) may lead to calcite dissolution and/or make the process of calcite formation (calcification) more difficult (Riebesell et al., 2000; Beaufort et al., 2011). Conflicting results concerning coccolithophore calcification have been reported from both experimental and field studies (e.g., Riebesell et al., 2000; Iglesias-Rodriguez et al., 2008; Riebesell and Tortell, 2011; Meyer and Riebesell, 2015). A recent study by Bach et al. (2015) found that laboratory findings could be reconciled when an optimum-type response to bicarbonate ion availability and pH where considered. In the field, different communities may respond to different combinations of elevated pH and/or nutrient availability, emphasizing the importance of species composition to community responses and to the multivariate nature of the growth environment (Poulton et al., 2011, 2014). Species-specific responses to ocean acidification are evident from laboratory work (Langer et al., 2006, 2009) and in the geological record (Gibbs et al., 2013; O'Dea et al., 2014), with regional oceanographic settings also having an important influence (Beaufort et al., 2011; Meier et al., 2014a). Hence, it is necessary to understand how coccolith (e.g. *E. huxleyi* strains in the SCS) size and morphology respond to environmental factors in the oligotrophic and marginal SCS.

In the present study, we performed an *in situ* investigation of coccolithophores (species composition, coccolith biometry) in the upper water-column of the South China Sea (SCS) in relation to the prevailing environmental conditions. The aims of this research were: (1) to examine coccolithophore biogeography more clearly alongside their calcite concentration in the upper water-column, and (2) to determine how coccolith morphology (i.e. *E. huxleyi*) responds to environmental variability (light, nutrients and carbonate chemistry) in a low-latitude marginal sea.

2 Materials and methods

2.1 Field sampling

A total of 72 water samples from 15 stations were collected during the R/V *Dongfanghong II* cruise of the National Science Foundation (2014). At most stations, five depths were sampled, including 25 m, 50 m, 75 m, 100 m and 150 m (Table 1). Water samples were not collected in the upper 5 m as this was extremely nutrient depleted, with especially low chlorophyll-*a*

concentrations (http://oceancolor.gsfc.nasa.gov/cms/) in summer (Fig. 1). For each water sample, 3 L was collected via a conductivity-temperature-depth (CTD) rosette sampler and filtered through 0.45 μm pore size 47 mm diameter nitrocellulose membrane filters (Sartorius®) under gentle pressure. The filters were rinsed to remove residual saline seawater, dried on an electric heat platform (65 ℃, 10-15 mins) and then stored in Petri dishes wrapped with aluminum foil and stored frozen (-20 °C).

2.2 Coccolithophore and coccolith counts

A small piece (~0.5 × 0.5 cm) of each filter was cut out and mounted on glass slides using Norland Optical Adhesive (No. 74). Coccolithophore cell counts and species identification was undertaken using cross-polarized light microscopy (Olympus BX51). In samples with abundant coccolithophore cells, individual cells (coccospheres) were counted from at least 100 field of views (FOV, diameter of each FOV is 220 μm) up to a total of 150 to 400 coccospheres. For samples with low abundance, around 50 extra FOVs were examined, which infers a detect limit of ~0.09 cells ml^{-1}. For counts and morphological measurements of detached coccoliths, a second piece of each filter was cut out (~0.5×0.5 cm) and mounted on an aluminum stub with double sided conductive carbon tape and coated with gold (see Poulton et al., 2011). A Leo 1450VP Scanning Electron Microscopy (Carl Zeiss) with SmartSEM (V5.1) software was then used to automatically capture images of consecutive FOVs from a 12×12 FOV (each FOV was 4.054×10^{-3} mm^2) grid at a magnification of ×5000, providing 144 images for analyses of detached coccolith counting and biometry. Coccolithophore species identification by light microscopy and Scanning Electron Microscopy (SEM) followed Frada et al. (2010), Young et al. (2003) and the Nannotax3 website (http://ina.tmsoc.org/Nannotax3/). Coccosphere and coccolith abundance was calculated using the following Eq. (1):

$$\text{Coccosphere/coccolith abundance (cells/coccoliths } ml^{-1}) = N \times S / (A \times V) \quad (1)$$

where N is the number of coccospheres or coccoliths counted, S is the filtered area (45 mm diameter) on each filter, A is the area inspected (A = number of FOV × area of 1 FOV), and V is the filtered water volume (ml).

2.3 Coccosphere and coccolith biometry and calcite estimates

Morphological parameters of *E. huxleyi* have been used to trace the influence of environmental conditions in field work (e.g. Poulton et al., 2011; Henderiks et al, 2012; Young et al., 2014). Two distinguishable morphotypes of *E. huxleyi* (type A and type B) were observed in the SEM images, with morphotype A generally comprising >90% of total *E. huxleyi* cell numbers. Hence, the measurements of *E. huxleyi* biometry including distal shield length (DSL) and coccospheres diameter (CD) were just based on morphotype A in this study. A total of 2560 *E. huxleyi* detached coccoliths (for DSL) and 102 intact coccospheres (for DSL and CD) were measured across the study sites.

Apart from *E. huxleyi*, coccolith lengths of all species were measured to estimate bulk coccolith calcite concentration in water-column. Individual coccolith calcite content (calcite mass) was calculated using Eq. (2) adapted from Young and Ziveri (2000), as in Poulton et al. (2011):

$$m \text{ (pg C, } CaCO_3) = 2.7 \times k_s \times DSL^3 \quad (2)$$

where 2.7 is density of calcite (pg C μm^{-3}), k_s is a shape constant determined for different species and DSL is the distal shield length of each coccolith (μm). For whole coccospheres, the calcite content was estimated by multiplying the calcite mass of a single coccolith (lying flat on the upper side of the coccosphere) with an estimate of the number of coccoliths in the coccosphere (e.g. 16 to 48 coccoliths in an *E. huxleyi* coccosphere in this study). Numbers of coccoliths per coccosphere in the present study were also estimated with reference to Boeckel and Baumann (2008). All the biometry works were performed from SEM images using ImageJ software (http://rsb.info.nih.gov/ij/), following Poulton et al. (2011).

Three coccolith species (*Gladiolithus flabellatus*, *Calciosolenia murrayi* and *Algirosphaera robusta*) present in the SCS do not have k_s values in Young and Ziveri (2000) or in similar coccolith calcite estimates (e.g., Knappertsbusch and Brummer,

1995; Beaufort and Heussner, 1999). For the body coccolith of *G. flabellatus*, a k_s value is estimated as 0.0016, adjusted from *Florisphaera profunda* (0.04) and based on their similar rectangle shapes. For *C. murrayi*, the rhomboid-shaped coccosphere is dimorphic, having both body coccoliths and narrow coccoliths around the apical opening (Young et al., 2003). Body coccolith lengths in *C. murrayi* range from 2.2 μm to 2.6 μm, with the mean length/width ratio ~3.045 in our samples, and the thickness is about 0.2 μm from Malinverno (2004). From these morphological parameters, the k_s value we estimated is 0.027. For *A. robusta*, each coccolith contains two parts: a base and a protrusion. The former is similar to a small *Syracosphaera* coccolith, with a k_s value of 0.015 (Young and Ziveri, 2000) and for the latter k_s value we calculated a cylindroid-like volume which we estimated as 0.045. Combining these two estimates gave a k_s value of 0.06 for *A. robusta* in this study.

2.4 Environmental parameters

Seawater temperature, salinity and chlorophyll fluorescence were taken from the CTD. For stations I4, I5, I6 and I7, CTD problems led to discontinuous temperature and salinity data. Mixed layer depths (MLD) were taken as the depth where the temperature difference was >0.5 ℃ with respect to surface waters (<5 m; Painter et al., 2010), while for stations I4 to I6, the MLD were only roughly determined according to vertical temperature profiles (see Fig. 2b). Euphotic zone depth is defined as the depth to which 1% of surface irradiance penetrates. Photosynthetically active radiation (PAR) through the water column is calculated following Eq. (3):

$$PAR_Z = PAR_0 \times \exp(-K_d \times Z) \quad (3)$$

where K_d, the vertical diffuse attenuation coefficient, is estimated by the following Eq. (4) from Wei (2005):

$$K_d = 0.027 + 0.252 \times c_p \quad (4)$$

where c_p is the beam attenuation recorded by the CTD. Identification of eddy activity was according to the temperature sections (Fig. 2) and altimeter data on sea level anomalies (SLA) and surface water flow from the AVISO website (http://www.aviso.altimetry.fr/en/home.html).

Macronutrient (nitrate+nitrite, phosphate) concentrations were determined immediately on board with colorimetric methods, using a Technicon AA3 Auto-Analyzer (Bran-Lube). The detection limits for nitrate+nitrite and phosphate are 0.1 μmol L^{-1} and 0.08 μmol L^{-1}, respectively. Seawater carbonate parameters (total alkalinity (A_T) and dissolved inorganic carbon (C_T)) were determined following the updated Joint Global Ocean Flux Study protocols (Dickson et al., 2007). Water samples for measurements were poisoned with saturated mercuric chloride solution and stored in dark before analysis. C_T was measured on board within 2 days of sampling and A_T was measured within two months. C_T was measured by collecting and quantifying the CO_2 released from the sample upon acidification with a non-dispersive infrared detector (Li-Cor® 7000). A_T was measured by potentiometric Gran titration. The accuracies of the A_T and C_T measurements were calibrated against the certified reference materials provided by A.G. Dickson of the Scripps Institution of Oceanography. Carbonate ion concentration, carbonate calcium saturation (Ω_C) and pH were calculated by CO_2SYS excel macro (Pierrot et al., 2006) from nutrients, C_T, A_T, temperature and salinity.

2.5 Statistical analysis

Multivariate data analysis were performed to further examine the coccolithophore composition across the study sites using PRIMER-E (v. 6.0) program (Clarke and Warwick, 2001). Before analysis, the sites of zero coccolithophore biomass and those at 150 m were removed and the absolute coccolithophore abundance data were then treated by square root-transformed. Bray-Curtis Similarity matrix was constructed with these coccolithophore biomass data and was analyzed via hierarchical cluster analysis (HCA) together with non-metric Multi-Dimensional Scaling (nMDS).

Principal component analysis was also performed based on the z-score normalized environmental parameters to evaluate the

main controlling factors. Pearson's product-moment correlations and Spearman's rank correlation were used to examine potential relationships between coccolithophore data and environmental factors. One-way ANOVA was performed to assess the coccolith length differences between samples. These statistical analyses were carried out using PAST software (Hammer et al., 2001).

3 Results

3.1 Physicochemical settings

A conspicuous deep chlorophyll-*a* maximum (DCM) was present throughout, ranging from 50 m to 75 m in depth (Fig. 3). Total nitrogen and phosphate concentrations were below the limit of quantitation in the upper 25 m, with the nutricline at a depth of ~50 m to 75 m (Fig. 3). All stations were stratified, with shallow mixed layers, ranging from 11 m to 35 m. According to the vertical temperature profiles, SLA map and geostrophic flows (Figs. 1b and 2), two anti-cyclonic eddies (labelled herein as AE) and one cyclonic eddy (CE) were present across the 18 ℃N section; with stations X4, X3 and J1 located in AE, F1 and D9 located in AE2, and I3 and H3 located in CE. The nutricline and DCM mirrored variability in the temperature profiles (Figs. 2 and 3), with shallowing in the upwelling CE, and deepening in the downwelling AE. Euphotic zone depths ranged from 90 m to 100 m, except at stations I1 and I2, where the euphotic zone was ~70 m depth. The detailed SLA and geostrophic flow maps during sampling dates can be found as supplementary figures.

3.2 Coccolithophore community

The average coccolithophore cell abundance was 11.82 cells ml^{-1}, ranging from <1 to 83.67 cells ml^{-1} across the sampling sites. The highest cell abundance was found at station I3 at a depth of 50 m. At each station, the lowest cell abundances were found at 25 m and/or 150 m, whereas the depths with the highest abundances was at 50 m and/or 75 m, in close proximity to the nutricline and DCM. A total of 17 coccolithophore taxa were counted (Table 2) across the study sites.

The nMDS ordination (Fig. 4) shows that at a level of 40% (dis)similarity in the HCA (see supplementary figures), three groups of water samples occurred: Group 1 mainly contained *E. huxleyi* and *Umbellosphaera irregularis*, with the lowest average cell concentrations of all the groups identified (8.57 cells ml^{-1}), and represented the shallowest samples (25 m and 50 m). Most of the samples were located at 25 m, and some at 50 m, (Fig. 5), and were representative of oligotrophic conditions in the upper mixed layer. Group 2 mainly was dominated by *E. huxleyi*, with the highest average cell concentration (27.38 cells ml^{-1}) of all the groups. Samples in this group were usually located at depths between 45 m and 75 m (Fig. 5), around 25 m below the MLD and representing the DCM, with elevated nutrients. Group 3 included taxa representing the lower photic zone (*A. robusta*, *F. profunda*), with *E. huxleyi* also abundant in most samples. Samples in Group 3 were found at 75 m and 100 m depth (Fig. 5) in which mean cell concentrations were 17.43 cells ml^{-1} and 9.04 cells ml^{-1}, respectively.

3.3 Estimates of coccolith and coccosphere calcite

The mean concentration of detached coccoliths was 158 coccoliths ml^{-1}, with a range from 0 to 673 coccoliths ml^{-1}. The highest detached coccolith concentration was observed at station F1 at 75 m, corresponding to the highest cells number (22.87 cells ml^{-1}) at this station. However, this pattern was not common at most stations where the depth of highest cell concentration rarely corresponded to the depth with the highest detached coccolith concentration. For example, the second highest detached coccolith concentration (623 coccoliths ml^{-1}) was found at station D9 at 150 m, the easternmost station sampled (Fig. 1), where coccosphere concentration was low (1.87 cells ml^{-1}). It is unlikely that such high abundances of detached coccoliths in deep layers of the water column could be produced *in situ* when cell abundances are so low, and hence these features may be characteristics of either lateral or vertical transport.

Based on coccosphere and detached coccolith concentrations, estimated total calcite concentrations ranged from <0.1 to 5258.1 pg C ml^{-1}, with a cruise average of 1508.3 pg C ml^{-1}. Estimated total calcite concentrations roughly mirrored detached coccolith concentrations (Fig. 6; Spearman's rank correlation, r_s = 0.81, p<0.01, n = 67), highlighting the contribution of detached coccoliths to particulate calcite in the water column. Our estimated calcite concentrations were in the same range as those estimated by Beaufort et al. (2008) in the southeast Pacific (2224 pg C ml^{-1} on average). The cruise average calcite concentrations based on three important coccolithophore species (*E. huxleyi*, *Gephyrocapsa oceanica* and *F. profunda*) who dominate surface sediments (Cheng and Wang, 1997; Fernando et al., 2007) and deep-sea coccolith fluxes (Jin et al., in prep.) in the SCS, were 273.0 pg C ml^{-1}, 112.1 pg C ml^{-1} and 391.3 pg C ml^{-1}, respectively. Their average relative contributions to water-column calcite were also estimated: *E. huxleyi* (17.04%), *G. oceanica* (7.00%) and *F. profunda* (24.42%) contributed to around half of water column calcite concentrations (Fig. 7). The depth distribution of these species contributions to total calcite matched well with their average depth distribution across the study area; *E. huxleyi* contributions were highest in the upper water column (25 m and 50 m), and *F. profunda* contributions were highest at depths of 75 m and 100 m.

3.4 Emiliania huxleyi biometry

From all the samples analyzed, the average distal shield length (DSL) of *E. huxleyi* type A was 2.96 μm, with an overall standard deviation of 0.39 μm. Pearson's product-moment correlations showed statistically significant relationships between average DSL, nutrients (nitrite+nitrate, phosphate), carbonate chemistry (pH, Ω_C and A_T) and temperature (T) (n = 29, Table 3). Statistically significant ($p < 0.01$) correlations occurred between DSL, total nitrogen (nitrite+nitrate) and phosphate (positive), and pH and Ω_C (negative), whereas no correlation occurred between DSL, A_T and T. The mean coccosphere diameter of *E. huxleyi* across all those measured was 6.41 μm, with a standard deviation of 0.95 μm. The average number of coccoliths estimated per coccosphere was 32, with an overall range from 16 to 48. Coccosphere diameter showed a statistically significant positive relationship with DSL (Pearson's r = 0.71, p<0.01, n = 102) and coccolith number per sphere (N) (Pearson's r = 0.51, p<0.01, n = 102). A binary regression equation gave coccosphere diameter = 1.205 × DSL + 0.106 × N + 0.096. Estimated coccosphere diameter predicted using this regression equation showed good agreement with that measured (y = 0.955 x, R^2 = 0.83).

4 Discussion

4.1 Coccolithophore biogeography in the South China Sea

In the context of the coccolithophore biogeographical zones of Winter et al. (1994), the coccolithophore assemblages investigated in the SCS belongs to the *tropical* zone, comprising *E. huxleyi*, *G. oceanica*, *G. ericsonii*, *O. fragilis*, *U. irregularis*, *F. profunda* and *A. robusta*. *Reticulofenestra sessilis* was also found in the SCS, and this species is exclusively found in the *tropical* zone where it may form symbioses with diatoms (i.e. *Thalassiosira* species) (Winter et al., 1994; Jordan, 2012). The coccolithophore flora of the SCS are similar with the "High Temperature" and "Warm Oligotrophic" assemblages in the equatorial Pacific Ocean (Hagino et al., 2000).

The two dominant species in our samples from the SCS were *E. huxleyi* and *F. profunda*, species representative of the upper and lower photic zone floral groups (Winter et al. 1994). These floral groups both live within the euphotic zone (>1% surface irradiance) which is about 100 m in summer in the SCS. However, in the West Pacific Warm Pool (stratified waters) and subtropical gyres of the Pacific and Atlantic Ocean, species *F. profunda* are found much deeper (150 m to 250 m) in the water-column (Hagino et al., 2000; Boeckel and Baumann, 2008; Beaufort et al., 2008). These differences are undoubtedly linked to differences between the SCS and open-ocean in terms of the depths of thermocline and nutricline, implying that the SCS is relatively eutrophic when compared with tropical and subtropical settings at a similar latitude.

Upper photic zone (UPZ) assemblage: In our nMDS analysis, the UPZ assemblage (Winter et al., 1994) was represented by Groups 1 and 2, found at 25 m and 50 m in the SCS. These two groups have different species composition in our analysis; for example, Group 1 included umbelliform species, such as *U. irregularis*, which are considered K-selected (specialists) species (Young, 1994) and agrees well with previous work (e.g. Okada and Honjo, 1975). The UPZ assemblage is commonly observed in well stratified, oligotrophic, warm surface waters in the West Pacific Warm Pool (Hagino et al., 2000). In the SCS, *U. irregularis* was mostly found at stations with deep mixed layers, deep nutriclines and extremely low nutrients in surface waters.

In comparison, Group 2 occurred at stations with shallower mixed layers and nutriclines, and hence potentially elevated nutrient supplies, and was more diverse, with *E. huxleyi* dominant. These results contradict with other studies in the SCS in summer, such as Okada and Honjo (1975) and Sun et al. (2011) who found that *G. oceanica* was the dominant species (30% to 100% of total cell numbers) in the western and southern parts of the SCS. Differences between this study and others could relate to the influence of the Asian summer monsoon on the western and southern SCS, where the southwesterly wind causes a wind driven upwelling system off the east coast of Vietnam (Liu et al., 2002; Xie et al., 2003; Ning et al., 2004). *G. oceanica* is considered a more eutrophic and coastal species (Andruleit and Rogalla, 2002; Andruleit et al., 2003) and hence it contributed less to coccolithophore biomass in the central and northern part of SCS, where summer monsoon induced upwelling/water mixing is weak.

Morphotype A was the dominant morphotype of *E. huxleyi* in the SCS. Different morphotypes of *E. huxleyi* can be distinguished by coccolith characteristics such as DSL, element widths and features of the central area (e.g., Young et al., 2003; Poulton et al., 2011), and may be considered as different ecotypes with different temperature and nutrient preferences (Cook et al., 2011; Poulton et al., 2011; Saavedra-Pellitero et al., 2014; Young et al., 2014). In our observations, the predominant occurrences of morphotype A could be related to high sea-surface temperature (>26ºC) of the tropical SCS. The southern part of SCS is also within the West Pacific Warm Pool, for which sea-surface temperature is >28 ℃ annually. In general, *E. huxleyi* type A shows a warmer water preference than type B and other type B derivatives (C, B/C). For instance, *E. huxleyi* type A and type B dominated in the warm Kuroshio and cold Oyashio currents, respectively, off Japan (Hagino et al., 2005). In the Pacific sector of the Southern Ocean, *E. huxleyi* type A was found in the sub-antarctic zone, while type B, C and B/C were found further south and colder waters (Saavedra-Pellitero et al., 2014).

Lower photic zone (LPZ) assemblage: In our study, the LPZ was represented by Group 3, which included typical LPZ species (*F. profunda*, *A. robusta* and *G. flabellatus*) and was found between 75 m and 100 m. Group 3 occurred above, at, or near the depth where 1% of surface irradiance penetrated (i.e., base of the euphotic zone). In other tropical oceans, the LPZ assemblage dwells deeper than the base of the euphotic zone (Hagino et al., 2000; Boeckel and Baumann, 2008; Beaufort et al., 2008). In the northern Arabian Sea, *F. profunda* inhabits shallower waters, and is found across a wider depth range (10 m to 80 m) (Andruleit et al., 2003). It is worth noting that, as in the SCS, the Arabian Sea is strongly controlled by a monsoonal system (Indian monsoon) and is considered relatively eutrophic (Andruleit and Rogalla, 2002; Andruleit et al., 2003). Hence, it can be inferred that neither water depth or light availability are limiting factors for *F. profunda* (and/or other LPZ species) in the SCS, but rather nutrient availability is important; the nitricline is shallow (50 m to 75 m) even in the oligotrophic summer in the SCS.

4.2 The response of coccolithophores to eddies in the South China Sea

Mesoscale eddies have a strong influence on productivity and ecosystem structure in the SCS (Chen et al., 2007b; Lin et al., 2010; Zhang et al., 2011). Previous measurements in the SCS have shown that integrated primary production in cyclonic eddies can be 2-3 fold higher relative to the outside of eddies (Chen et al., 2007b). Modelling results have also highlighted how new production, relative to outside of eddies, can be ~30% higher or lower in cyclonic or anti-cyclonic eddies, respectively (Xiu and Chai, 2011).

With further examination of the nMDS, HCA and eddy settings in the 18°N section, it is clear that the coccolithophore communities in the SCS were strongly coupled with eddy occurrences (Fig. 5). In the cyclonic) eddy (I3, H3), Group 2 occurred in ranges from 25 m to 50 m depth and Group 3 occurred within layers from 75 m to 100 m. Comparatively, at stations (X5, G2) with "normal" (non-eddy) conditions, three groups sequentially occurred in the water-column; Group 1 at 25 m, Group 2 at 50 m and Group 3 between 75 m to 100 m depth. In anti-cyclonic eddies, there were two patterns: one with Group 1 distributed within a wider depth range (from 25 to 50 m), and Group 3 was just within a 100 m layer; another was that Group 2 was absent, and the coccolithophore maximum layers were in Group 3, which was dominated by LPZ assemblages (e.g. *F. profunda*). This transition highlights the importance of ecological effects of eddies on the coccolithophore community's depth distribution through the water-column. As the anti-cyclonic eddy (cyclonic eddy) centers are convergence (divergence) of the adjacent waters, deepening (shallowing) the nutricline and making the water-column more oligotrophic (slightly eutrophic), conditions which favor distinct coccolithophore assemblages (Fig. 8).

Due the discontinuous sampling dates (Table 1) and low resolution of environmental data at some stations, the meridional section may not be suitable for assessing the eddy impacts on coccolithophore communities. For example, at I6 and I7 stations were not characteristic of anti-cyclonic eddies based on the SLA and geostrophic flow map, however, the coccolithophore community locations are similar to those in the anti-cyclonic eddies. This may be due to the deeper nutricline in the central basin of the SCS, even if the water-column structure had not been modulated by eddies in our investigation. Another example is stations I1 and I2, for which the coccolithophore groups agreed with those in the cyclonic eddies. Likewise, this was also not characteristic of the cyclonic eddies, as shown by SLA and geostrophic flow (supplementary figures). At stations I1 and I2, the euphotic zone depth was relatively shallow (~70 m), with more light attenuation from suspended particles, which could be caused by elevated particle production. This finding corresponds with the station locations at the edge of the anti-cyclonic eddy where particulate organic carbon (POC) fluxes can be 2 to 4 folder higher than those in adjacent oligotrophic waters (Zhou et al., 2013; Shih et al., 2015). The case for station I4 was similar to I1 and I2, as it was located at the edge of two large anti-cyclonic eddies (supplementary figures). The horizontal advection, for water mass balance, can result in the elevated nutricline in anti-cyclonic eddy edges, and hence, the enhancement of POC production and export (Zhou et al., 2013).

Station I5 had another distinctive arrangement of species assemblages which was opposite to that found at the other stations sampled (Fig. 5); Group 2 was found at 25 m while Group 1 was at 50 m. Examination of the temperature profile shows that the 29.5℃ isotherm was shallow and domed, while the 22.5℃ isotherm was pushed deeper into the water column (Fig. 2b). Filters collected at 25 m and 50 m from I5 also had lots of diatom fragments, and relatively elevated coccolithophore abundances (21.75 and 22.59 cells ml^{-1} in 25 and 50 m, respectively). We suggest that this feature may represent a mode-water eddy, as described by McGillicuddy et al. (2007) in the northeast subtropical Atlantic Ocean. McGillicuddy et al. (2007) observed elevated phytoplankton production (i.e. a diatom bloom) in a mode-water eddy, which led to local changes in the zooplankton community composition (McGillicuddy et al., 2007; Eden et al., 2009).

4.3 Calcite concentrations in the South China Sea

The discrete estimates of bulk coccolith calcite roughly co-varied with coccolith and coccolithophore concentration in the water-column, with peak concentrations around the DCM. Rather than controlled by the environmental factors (light, nutrients, carbonate chemistry), the vertical distribution of bulk coccolith calcite reflected changes in the coccolithophore community composition. For example, the specific calcite contribution of *E. huxleyi* and *F. profunda* reflected the coccolithophore community changes through the water-column. They contributed more to calcite in the cyclonic eddy and less in the anti-cyclonic eddies. In addition, excluding the maximum calcite concentration in the DCM, another peak was also found in deeper water at some stations, for example at 150 m in F1 and D9, and 100 m and 150 m in I7 station, where the cell concentrations were low and calcite was nearly all contributed by detached coccoliths.

E. huxleyi, G. oceanica and F. profunda represented around half of the calcite in the water column (Fig. 7), whereas other species with smaller levels of abundance contribute to the other 50% of water-column calcite. The greater contribution of these relatively less abundant species in calcite inventories is partly related to higher per coccolith calcite contents, due in part to larger coccolith lengths (Young and Ziveri, 2000); for example, *O. fragilis* has >80 pg C per coccolith whereas *E. huxleyi* has ~2 pg C per coccolith. Relatively rare coccolithophore species with high coccolith and coccosphere calcite contents are important vectors of both upper-ocean calcite production (Daniels et al., 2014) and deep-sea calcite fluxes (Ziveri et al., 2007). However, examination of sediment trap material (500 m depth, 1500 m above the sea floor) in the northern SCS basin shows that these three species (*E. huxleyi, G. oceanica and F. profunda*) dominating upper ocean calcite inventories all have an increased contribution to coccolith (>95%) and coccolith calcite (>85%) fluxes (Jin et al., in prep.). This highlights the discrepancy between coccolith calcite in the euphotic zone and aphotic deep ocean. Notably, at 150 m for some stations (D9, F1, G2, I5, X3), these three species can totally comprise more than 70% to 90% of calcite inventories and the contribution of *G. oceanica* exceed those of *E. huxleyi* (Fig. 7), which is similar to the fluxes of sediments of moored traps. One possible reason is that these coccoliths are attributed to lateral transport of the nepheloid layer originated from continental shelf or slope. This is most likely the case for D9 and F1 stations, as they have such high detached coccolith concentrations (Fig. 6) and are located in the westernmost of the 18 °N section. Alternatively, coccoliths in the deep layer are a result from vertical sinking. It indicates that the higher contribution of these species in the deep layer may result from their higher production rate in the photic zone, which cannot be reflected from the snapshot-like discrete sampling done in our study.

4.4 Environmental influences on Emiliania huxleyi biometry

Nutrients and light: Some culture experiments have shown that nutrients may exert little influence on coccolith calcification rate or morphological variance (Paasche, 1998; Fritz, 1999; Langer and Benner, 2009; Langer et al., 2012). In mesocosm enclosures coccolith size has been shown to change under low phosphate conditions (Båvik et al., 1997; Engel et al., 2005). A culturing study of *E. huxleyi* strains isolated from the Mediterranean Sea showed an increase in coccosphere size and cell calcite content under phosphorus limitation (Oviedo et al., 2014). These different results of *E. huxleyi* calcite quota or calcification rate under nutrient limitation may actually result from strain-specific physiological responses (Oviedo et al., 2014). A detailed model has recently highlighted how nitrogen and phosphorus are required for distinctly different cellular usages, nitrogen for biomass growth and phosphorus for cell division and organic maturity (Aloisi, 2015). Phosphorus limitation delays cell division, whereas coccolithophore can still divide when nitrogen is not limiting, hence cellular particulate inorganic carbon (PIC) increases under phosphorus stress (Müller et al., 2008; Aloisi, 2015). In the present study, a positive relationship between nutrients (both nitrogen and phosphorus) and *E. huxleyi* coccolith size was found (Table 3). Actually, the largest coccoliths occurred at the deepest depths where nutrient was sufficient and light was insufficient, while within the *E. huxleyi* abundant layer coccoliths were relatively small (most remarkable at X3, F1, D9, I7, X5, Fig. 9a).

If nutrients are the only limiting factor in *E. huxleyi* growth (i.e. under laboratory culturing conditions), when nutrients are replete, *E. huxleyi* growth is fast (exponential phase), with fewer and smaller coccoliths per cell. When nutrients become limiting, *E. huxleyi* growth slows (stationary phase), and larger and multi-layer coccospheres are produced (Gibbs et al., 2013). A culturing experiment of *E. huxleyi* strain NIES 837 has shown that during rapid cell division, coccoliths production on cells ceased (Satoh et al., 2009). In our case in the SCS (in field conditions), nutrients were not the only limiting factor influencing *E. huxleyi* growth. We propose that light is also a strong limiting factor for *E. huxleyi* production and calcification in natural communities (Poulton et al., 2014). However, some authors have stated that light should not be regarded as a factor regulating phytoplankton growth in the oligotrophic SCS as the euphotic zone depth exceeds the MLD and nutricline throughout the year (Tseng et al., 2005; Wong et al., 2007). Here, we propose a simple schematic (Fig. 9b): we suggest that nutrients are not limiting below the nutricline. (1) In the DCM layer, when light and nutrients are optimal for

phytoplankton growth, *E. huxleyi* growth is fast and they produce small sized coccoliths; (2) In deeper waters, when nutrients are more sufficient but light is not available, *E. huxleyi* growth slows and they produce larger sized coccoliths. That light limitation, in *E. huxleyi* cells, can prolong G1 assimilation stage during which calcification takes place will at last increase cellular calcite content (Müller et al., 2008); (3) Above the nutricline, when light is sufficient and nutrients are depleted, it is possible that *E. huxleyi* coccolith size is depended on whether inorganic phosphorus is deficient or organic phosphorus compounds can be utilized, although we lack data to directly address either nutrient availability or coccolith biometry in these samples.

The same trend of calcification in the water column has also been found off the Loffoten Islands in the Norwegian Sea (Charalampopoulou et al., 2011). Cell calcification rate was <1 pmol C $cell^{-1}$ d^{-1} in the coccolithophore maximum layer, while it was about three times higher in upper and lower waters where coccolithophores were less abundant (Charalampopoulou et al., 2011), although bulk calcification in their study was influenced by light and coccolithophore species composition (Charalampopoulou et al., 2011). That opposite results were found in Benguela coastal upwelling system where coccospheres and coccoliths in the DCM (~17 m) were larger than those at 50 m depth could be due to different bloom/growth stages of *E. huxleyi* (Henderiks et al., 2012). Largest coccoliths/coccospheres were reported in late exponential growth stage (11^{th} day) in mesocosm experiments (Engel et al., 2005). With a closer inspection, in their experiments phosphate was exhausted at the 11^{th} day (<0.05 μmol L^{-1}), while nitrate was not below detection limits until 13^{th} day (Engel et al., 2005). It means that phosphorus limitation regulated growth rate (decrease) with co-variation of cellular calcification (increase, negative response) (Müller et al., 2008; Aloisi, 2015). However, it is not the case in the SCS, because both nutrients were replete at deeper depths, and growth rate was, we suggested, limited by light availability. Other contrary results came from sediment traps which showed that heaviest coccolith weight of *E. huxley*i was linked to primary productivity in bloom seasons in the tropical Atlantic and the Mediterranean Sea (Beaufort et al., 2007; Meier et al., 2014b). Nevertheless, these changes may account for the seasonal succession of heavily and lightly calcified *E. huxleyi* (possibly different morphotypes) (Triantaphyllou et al., 2010; Meier et al., 2014b).

Coccolithophore calcification rates of natural communities are strongly light-dependent (e.g., Poulton et al., 2007, 2010, 2014; Charalampopoulou et al., 2011), although it may seem paradoxical that light availability regulates coccolithophore growth rates while light limitation can increase cellular levels of calcite (e.g., Paasche, 2001; Rost and Reibesell, 2004; Müller et al., 2008). Calcification (and photosynthetic) rates may be simplified to growth rate (μ) × PIC (POC) $cell^{-1}$, where light and/or nutrient limitation may lower μ. Hence, calcification and photosynthetic rates are both influenced by μ (to large extent), and will obviously show strongly coupled relationships to limiting factors. However, the cellular PIC or POC content may also increase when light and/or nutrients such as phosphorus are limiting (Müller et al., 2008; Aloisi, 2015). Thus, this paradox may come about from the different perspectives on coccolith calcification (rate). Overall, cell/coccolith size and cell calcification rate variations are a combination of physiological responses to environmental constraints.

Temperature: Temperature should be a critical factor for coccolithophore growth and cell size. An *E. huxleyi* strain isolated from Greet Barrier Reef showed an optimal growth temperature at 25 ℃ with the smallest cell size, while the growth rate and cell size got lower and bigger in parallel as the temperature was decreased to 10 ℃ (Sorrosa et al., 2005). A recent culturing study (Saruwatari et al., 2016) has also shown that *E. huxleyi* strains of morphotype B/C isolated from the Arctic Ocean grow faster and produce smaller coccoliths when temperature increases from 5 ℃ to 20 ℃. However, contradictory results come from Rosas-Navarro et al. (2016), who have found that *E. huxleyi* (type A, strains isolated from North Pacific Ocean) produce the largest coccoliths within the optimal growth temperature of 20 ℃ to 25 ℃. Apparently, these different patterns of *E. huxleyi* coccolith size may result from strain-specific or morphotype (ecotype) responses to temperature. In the present study, temperature was not found to correlate with *E. huxleyi* coccolith size from the statistical analysis (Table 3). One possible reason could be that the temperature profiles were to large extent controlled by the eddy related water-column structure (i.e. MLD), which may possibly mute the signal of their influences on *E. huxleyi* growth and size. Alternatively, as

stated by Bach et al. (2012), temperature may exert little physiological influence on *E. huxleyi* size. In addition, the temperature at the investigated stations ranged from 18 ℃ to 25 ℃ at depths from 100 m to 50 m, which is near the optimal growth temperature for many *E. huxleyi* strains (20 ℃ to 25 ℃; Paasche, 2001; Sorrosa et al., 2005; Rosas-Navarro et al., 2016). That is, temperature may not be a limiting factor for *E. huxleyi* growth within the euphotic zone in the tropical SCS, apart from surface and/or near-surface waters where water temperatures are >29 ℃, above the growth optimum temperature range for this species (Rosas-Navarro et al., 2016).

Carbonate chemistry: Coccolithophores are thought to be sensitive indicators of carbonate chemistry, especially Ω_C and [CO_3^{2-}] (e.g., Beaufort et al., 2011). Our results show an inverse correlation between DSL and pH, and Ω_C. Similarly, *E. huxleyi* calcification has been found to be negatively correlated with Ω_C in the shelf waters of the Northwest European shelf (Poulton et al., 2014). In their case, the range in Ω_C and pH values were small compared with many open-ocean situations (Poulton et al., 2014). In our case, all the environmental data was significantly inter-correlated (Table 3), nearly all contributing to one principal component (PC-1, 76.59% of variance) (Table 3). That is, the environmental gradients in the water-column are depended on sampling depth. Importantly, in the data from the SCS the carbonate chemistry inversely mirrors the nutrient data, making it hard to distinguish its influence on coccolith morphology. Hence, it is not possible to directly infer that *E. huxleyi* calcification and carbonate chemistry have a simple cause and effect relationship in the SCS.

Here, our DSL results in the SCS were compared with those in the North Sea (Young et al., 2014) (Fig. 10). In the North Sea, *E. huxleyi* was also dominated by morphotype A (Young et al., 2014). While Ω_C in the two regions falls within a similar range, DSL shows a significant difference ($F = 17.18$, $p<0.01$). The morphotype in both the North Sea and SCS was A, and hence what causes the morphological distinction may be genotypic variation or an "*ecological*" effect (Bach et al., 2012). It is suggested that the changing environmental conditions can select for different coccolithophore strains, which indirectly influences the coccolith size and morphology (Bach et al., 2012). For example, different environmental provinces can shift from a community dominated by normally calcified *E. huxleyi* type A to one characterized by weakly calcified B/C on the Patagonian Shelf and Southern Ocean (Cubillos et al., 2007; Poulton et al., 2011). Heavier calcified morphotypes during low Ω_C in winter may be responsible for the seasonal morphotype transition in the Bay of Biscay (Smith et al., 2012). Seasonal variability of *E. huxleyi* coccolith size has also been observed in the Aegean Sea, which may be due to genotypic or ecophenotypic variation (Triantaphyllou et al., 2010). Additionally, Young et al. (2014) have argued that *E. huxleyi* DSL differences relate to neritic and oceanic groups rather than carbonate chemistry impacts. DSL in our samples show no significant difference with those in the oceanic group ($F = 0.243$, $p = 0.63$), however, they are significantly lower than those in the neritic group from Young et al. (2014) ($F = 125.2$, $p<<0.01$) (Fig. 10). Meier et al. (2014a) found that mean coccolith weight peaked at the Rockall Plateau during Heinrich event 11, when Ω_C and pH had low values. This could be due to a coccolith assemblage shift to heavier calcified morphotypes with relation to oceanic frontal changes during this geological episode rather than carbonate chemistry variations (Meier et al., 2014a). Hence, the ecological transition of assemblages may be a more dominant effect on coccolith morphology and/or cellular calcification in not only the present ocean, but also in geological records.

5 Conclusions

In the South China Sea (SCS), the coccolithophore community corresponds to the tropical biogeographic zone, with many characteristic tropical species being present (e.g., *Umbellosphaera irregularis*, *Florisphaera profunda*). Coccolithophore cellular abundances ranged from <1 cells ml^{-1} to 83.67 cells ml^{-1} across the SCS basin. Highest cell concentrations occurred in the DCM, with all of the coccolithophore community within the euphotic zone (i.e. above the depth where 1% of surface irradiance penetrates). *Emiliania huxleyi* (type A) was the numerically dominant species in the SCS during summer.

Water samples were divided into 3 groups according to the composition of their coccolithophore communities. Group 1, characterised by the presence of *U. irregularis*, preferred oligotrophic conditions; Group 2, dominated by *E. huxleyi*, had

relative high coccolithophore cell abundances; and Group 3 contained lower photic species such as *F. profunda*. These coccolithophore communities through the water-column showed strong vertical differentiation, with depth shifts in response to mesoscale eddy features along the 18 ℃N section (Fig. 5, Fig. 8). Briefly, anti-cyclonic eddies were occupied with oligotrophic representative species, whereas coccolithophore assemblages in the cyclonic eddy were represented by more eutrophic and slightly productive flora.

Estimates of calcite concentrations in the upper water column based on coccosphere and coccolith calcite contents closely matched detached coccolith concentrations highlighting their significant contribution to calcite standing stocks. Three key species (*E. huxleyi*, *Gephyrocapsa oceanica*, *F. profunda*) contributed roughly half (Fig. 7) of the surface ocean coccolith-calcite concentrations. Moreover, they had an increased contribution to deep sea coccolith and calcite fluxes (Jin et al., in prep.), highlighting their importance for coccolith carbonate production in the SCS.

Biometric measurements of *E. huxleyi* coccoliths showed significant ($p<0.01$) positive relationships with nutrient (nitrate, phosphate) concentrations and negative relationships with carbonate chemistry (pH, Ω_C) (Table 3), although all of these environmental parameters were strongly correlated. It is suggested that light and nutrients are more likely to explain the *E. huxleyi* coccolith variations rather than carbonate chemistry. As larger sized coccoliths for *E. huxleyi* are produced in deep and light limited waters with slow cell growth rate, while in optimal conditions (i.e. in deep chlorophyll maximum), they are likely to produce smaller sized coccoliths with faster growth rates.

Author contributions

X.B.J., C.L.L. and A.J.P. designed the experiments and X.B.J. carried them out. C.L.L. was the supervisor of this project. X.B.J. and A.J.P. drafted and revised the manuscript. Nutrients and carbonate chemistry data were provided by M.H.D. and X.H.G.

Acknowledgements

This work is financed by the National Natural Science Foundation of China (grants 91228204, 41376047). We are grateful to the cruise colleagues of R/V *Dongfanghong II* and the Ocean Carbon Group of Xiamen University. We are also grateful to R.B. Pearce, R.M. Sheward and G.M. Fragoso for their assistance in light and scanning electron microscopy, and H.E.K. Smith for her assistance in statistical analysis (National Oceanography Centre). M. Wang and H.R. Zhang are thanked for their assistance in Aviso data compiling. A.J. Poulton would also like to acknowledge financial support from National Capability funding from the Natural Environmental Research Council. We also thank the anonymous reviewers for their constructive comments on the discussion paper.

References

Aloisi, G.: Covariation of metabolic rates and cell size in coccolithophores. Biogeosciences, 12(15), 6215-6284. 2015.

Andruleit, H., Rogalla, U.: Coccolithophores in surface sediments of the Arabian Sea in relation to environmental gradients in surface waters. Marine Geology, 186(3), 505-526. 2002.

Andruleit, H., Stäger, S., Rogalla, U., Čepek, P.: Living coccolithophores in the northern Arabian Sea: ecological tolerances and environmental control. Marine Micropaleontology, 49(1), 157-181. 2003.

Bach, L.T., Bauke, C., Meier, K.J.S., Riebesell, U., Schulz, K. G.: Influence of changing carbonate chemistry on morphology and weight of coccoliths formed by *Emiliania huxleyi*. Biogeosciences. 9(8), 3449-3463. 2012.

Bach, L.T., Riebesell, U., Gutowska, M.A., Federwisch, L., Schulz, K.G.: A unifying concept of coccolithophore sensitivity to changing carbonate chemistry embedded in an ecological framework. Progress in Oceanography, 135, 125-138. 2015.

Balch, W.M., Holligan, P.M., Ackleson, S.G., Voss, K.J.: Biological and optical properties of mesoscale coccolithophore blooms in the Gulf of Maine. Limnology and Oceanography, 36(4), 629-643. 1991.

Balch, W.M., Drapeau, D.T., Bowler, B.C., Lyczkowski, E.R., Booth, E.S., Alley, D.: The contribution of coccolithophores to the optical and inorganic carbon budgets during the Southern Ocean Gas Exchange Experiment: New evidence in support of the "Great Calcite Belt" hypothesis. Journal of Geophysical Research: Oceans (1978–2012), 116(C4). 2011.

Balch, W.M., Drapeau, D.T., Bowler, B.C., Lyczkowski, E.R., Lubelczyk, L.C., Painter, S.C., Poulton, A.J.: Surface biological, chemical, and optical properties of the Patagonian Shelf coccolithophore bloom, the brightest waters of the Great Calcite Belt. Limnology and Oceanography, 59(5): 1715-1732. 2014.

Båtvik, H., Heimdal, B.R., Fagerbakke, K.M., Green, J.C.: Effects of unbalanced nutrient regime on coccolith morphology and size in *Emiliania huxleyi* (Prymnesiophyceae). European Journal of Phycology, 32(02), 155-165. 1997.

Beaufort, L., Heussner, S.: Coccolithophorids on the continental slope of the Bay of Biscay–production, transport and contribution to mass fluxes. Deep Sea Research Part II: Topical Studies in Oceanography. 46(10): 2147-2174. 1999.

Beaufort, L., Probert, I., Buchet, N.: Effects of acidification and primary production on coccolith weight: implications for carbonate transfer from the surface to the deep ocean. Geochemistry Geophysics Geosystems, 8(8), 582-596. 2007.

Beaufort, L., Couapel, M., Buchet, N., Claustre, H., Goyet, C.: Calcite production by coccolithophores in the south east Pacific Ocean. Biogeosciences, 5(4): 1101-1117. 2008.

Beaufort, L., Probert, I., Garidel-Thoron, T., Bendif, E.M., Ruiz-Pino, D., Metzl, N., Goyet, C., Buchet, N., Coupel, P., Grelaud, M., Rost, B., Rickaby, E.M., Vargas, C.: Sensitivity of coccolithophores to carbonate chemistry and ocean acidification. Nature, 476(7358): 80-83. 2011.

Boeckel, B., Baumann, K.H.: Vertical and lateral variations in coccolithophore community structure across the subtropical frontal zone in the South Atlantic Ocean. Marine Micropaleontology, 67(3): 255-273. 2008.

Borgne, L.R., Barber, R.T., Delcroix, T., Inoue, H.Y., Mackey, D.J., Rodier, M.: Pacific warm pool and divergence: temporal and zonal variations on the equator and their effects on the biological pump. Deep Sea Research Part II: Topical Studies in Oceanography, 49(13), 2471-2512. 2002.

Charalampopoulou, A., Poulton, A.J., Tyrrell, T., Lucas, M.I.: Irradiance and pH affect coccolithophore community composition on a transect between the North Sea and the Arctic Ocean. Marine Ecology Progress Series, 431, 25-43. 2011.

Chen, C.C., Shiah, F.K., Chung, S.W., Liu, K.K.: Winter phytoplankton blooms in the shallow mixed layer of the South China Sea enhanced by upwelling. Journal of Marine Systems, 59(1): 97-110. 2006.

Chen, G., Hou, Y., Chu, X.: Mesoscale eddies in the South China Sea: Mean properties, spatiotemporal variability, and impact on thermohaline structure. Journal of Geophysical Research: Oceans (1978–2012), 116(C6). 2011.

Chen, Y.L.: Spatial and seasonal variations of nitrate-based new production and primary production in the South China Sea. Deep Sea Research Part I: Oceanographic Research Papers, 52(2): 319-340. 2005.

Chen, Y.L., Chen, H.Y., Chung, C.W.: Seasonal variability of coccolithophore abundance and assemblage in the northern South China Sea. Deep Sea Research Part II: Topical Studies in Oceanography, 54(14): 1617-1633. 2007a.

Chen, Y.L., Chen, H.Y., Lin, I.I., Lee, M.A., Chang, J.: Effects of cold eddy on phytoplankton production and assemblages in Luzon Strait bordering the South China Sea. Journal of oceanography, 63(4): 671-683. 2007b.

Cheng, X.R., Wang, P.X.: Controlling factors of coccolith distribution in surface sediments of the China seas: marginal sea nannofossil assemblages revisited. Marine Micropalontology, 32: 155-172. 1997.

Clarke, K.R. and Warwick, R.M.: Change in marine communities: an approach to statistical analysis and interpretation, 2nd edition. PRIMER-E: Plymouth. 2001.

Cokacar, T., Oguz, T., Kubilay, N.: Satellite-detected early summer coccolithophore blooms and their interannual variability in the Black Sea. Deep Sea Research Part I: Oceanographic Research Papers, 51(8), 1017-1031. 2004.

Cook, S.S., Whittock, L., Wright, S.W., Hallegraeff, G.M.: Photosynthetic pigment and genetic differences between two Southern Ocean morphotypes of *Emiliania huxleyi* (Haptophyta). Journal of Phycology, 47(3), 615-626. 2011.

Cubillos, J.C., Wright, S.W., Nash, G., De Salas, M.F., Griffiths, B., Tilbrook, B., Poisson, A., Hallegraeff, G.M.: Calcification morphotypes of the coccolithophorid *Emiliania huxleyi* in the Southern Ocean: changes in 2001 to 2006 compared to historical data. Marine Ecology Progress Series, 348, 47-54. 2007.

Daniels, C.J., Sheward, R.M., Poulton, A.J.: Biogeochemical implications of comparative growth rates of *Emiliania huxleyi* and Coccolithus species. Biogeosciences, 11(23), 6915-6925. 2014.

Dickson, A.G., Sabine, C.L., Christian, J.R. Guide to best practices for ocean CO_2 measurements. PICES Special Publication 3, 191 pp. 2007.

Eden, B.R., Steinberg, D.K., Goldthwait, S.A., McGillicuddy, D.J.: Zooplankton community structure in a cyclonic and mode-water eddy in the Sargasso Sea. Deep Sea Research Part I: Oceanographic Research Papers, 56(10), 1757-1776. 2009.

Engel, A., Zondervan, I., Aerts, K., Beaufort, L., Benthien, A., Chou, L., Delille, B., Gattuso, J., Harlay, J., Heemann, C., Hoffmann, L., Jacquet, S., Nejstgaard, J., Pizay, M., Rochelle-Newall, E., Schneider, U., Terbrueggen, A., Riebesell, U.: Testing the direct effect of CO_2 concentration on a bloom of the coccolithophorid *Emiliania huxleyi* in mesocosm experiments. Limnology and Oceanography, 50(2), 493-507. 2005.

Fernando, A.G.S., Peleo-Alampay, A.M., Wiesner, M.G.: Calcareous nannofossils in surface sediments of the eastern and western South China Sea. Marine Micropaleontology, 66(1): 1-26. 2007.

Frada, M., Young, J., Cachão, M., Lino, S., Martins, A., Narciso, Á., Probet, I., de Vargas, C.: A guide to extant coccolithophores (Calcihaptophycidae, Haptophyta) using light microscopy. Journal of Nannoplankton Research, 31, 58-112. 2010.

Fritz, J.J., Carbon fixation and coccolith detachment in the coccolithophore *Emiliania huxleyi* in nitrate-limited cyclostats.: Marine Biology, 133(3), 509-518. 1999.

Gibbs, S.J., Poulton, A.J., Bown, P.R., Daniels, C.J., Hopkins, J., Young, J.R., Jones, H.L., Thiemann, G.J., O'Dea, S.A., Newsam, C.: Species-specific growth response of coccolithophores to Palaeocene-Eocene environmental change. Nature Geoscience, 6(3), 218-222. 2013.

Hagino, K., Okada, H., Matsuoka, H.: Spatial dynamics of coccolithophore assemblages in the Equatorial Western-Central Pacific Ocean. Marine Micropaleontology, 39(1): 53-72. 2000.

Hagino, K., Okada, H., Matusoka, H.: Coccolithophore assemblages and morphotypes of *Emilania huxleyi* in the boundary zone between the cold Oyashio and warm Kuroshio currents off the coast of Japan. Marine Micropaleontology, 55(1):119-47. 2005.

Hammer, Ø., Harper, D.A. T., Ryan, P.D.: PAST: Paleontological Statistics Software Package for education and data analysis. Palaeontolia Electronica 4. 2001.

Henderiks, J., Winter, A., Elbrächter, M., Feistel, R., Van der Plas, A., Nausch, G., Barlow, R.: Environmental controls on *Emiliania huxleyi* morphotypes in the Benguela coastal upwelling system(SE Atlantic). Marine Ecology Progress Series, 448, 51-66. 2011.

Hu, J., Gan, J., Sun, Z., Zhu, J., Dai, M.H., Observed three‐dimensional structure of a cold eddy in the southwestern South China Sea. Journal of Geophysical Research: Oceans (1978–2012), 116(C5). 2011.

Huang, B., Hu, J., Xu, H., Cao, Z., Wang, D.: Phytoplankton community at warm eddies in the northern South China Sea in winter 2003/2004. Deep Sea Research Part II: Topical Studies in Oceanography, 57 (19), 1792-1798. 2010.

Iglesias-Rodriguez, M.D., Halloran, P.R., Rickaby, R.E.M., Hall, I.R., Colmenero-Hidalgo, E., Gittins, J.R., Green, D.R.H., Armbrust, E.V., Boessenkool, K.P.: Phytoplankton calcification in a high-CO_2 world. Science, 320(5874): 336-340. 2008.

Jordan, R.W.: Coccolithophores. In Eukaryotic Microbes, edited by Schaechter, M., Elsevier. 2012.

Knappertsbusch M, Brummer G.J.A.: A sediment trap investigation of sinking coccolithophorids in the North Atlantic. Deep Sea Research Part I: Oceanographic Research Papers, 42(7): 1083-1109. 1995.

Langer, G., Geisen, M., Baumann, K.H., Klä̈s, J., Riebesell, U., Thoms, S., Young, J.R.: Species−specific responses of calcifying algae to changing seawater carbonate chemistry. Geochemistry, Geophysics, Geosystems, 7(9). 2006.

Langer, G., Benner, I.: Effect of elevated nitrate concentration on calcification in *Emiliania huxleyi*. Journal of Nannoplankton Research, 30, 77-80. 2009.

Langer, G., Nehrke, G., Probert, I., Ly, J., Ziveri, P.: Strain-specific responses of *Emiliania huxleyi* to changing seawater carbonate chemistry. Biogeosciences, 6(11): 2637-2646. 2009.

Langer, G., Oetjen, K., Brenneis, T.: Calcification of *Calcidiscus leptoporus* under nitrogen and phosphorus limitation. Journal of Experimental Marine Biology and Ecology, 413, 131-137. 2012.

Liu, K.K., Chao, S.Y., Shaw, P.T.: Gong, G.C., Chen, C.C., Tang, T.Y. Monsoon-forced chlorophyll distribution and primary production in the South China Sea: observations and a numerical study. Deep Sea Research Part I: Oceanographic Research Papers, 49(8), 1387-1412. 2002.

Malinverno, E.: Morphological variability within the genus *Calciosolenia* (coccolithophorids) from the eastern Mediterranean Sea. Micropaleontology, 81-91. 2004.

McGillicuddy, D.J., Anderson, L.A., Bates, N.R., Bibby, T., Buesseler, K.O., Carlson, C.A., Davis, C.S., Ewart, C., Falkowski, P.G., Goldthewait, S.A., Hansell, D.A., Jenkins, W.J., Johnson, R., Kosnyrev, V.K., Ledwell, J.R., Li, Q.P., Siegel, D.A., Steinberg, D.K.: Eddy/wind interactions stimulate extraordinary mid-ocean plankton blooms. Science, 316(5827), 1021-1026. 2007.

Meier, K.J.S., Berger, C., Kinkel, H.: Increasing coccolith calcification during CO_2 rise of the penultimate deglaciation (Termination II). Marine Micropaleontology, 112: 1-12, 2014a.

Meier, K.J.S., Beaufort, L., Heussner, S., Ziveri, P.: The role of ocean acidification in *Emiliania huxleyi* coccolith thinning in the Mediterranean Sea. Biogeosciences, 11(10), 2857-2869. 2014b.

Meyer, J., Riebesell, U.: Reviews and syntheses: responses of coccolithophores to ocean acidification: a meta-analysis. Biogeosciences, 12(6), 1671-1682. 2015.

Müller, M., Antia, A., LaRoche, J.: Influence of cell cycle phase on calcification in the coccolithophore *Emiliania huxleyi*. Limnology and Oceanography, 53(2), 506-512. 2008.

Ning, X.R., Chai, F., Xue, H., Cai, Y., Liu, C., Shi, J.: Physical‐biological oceanographic coupling influencing phytoplankton and primary production in the South China Sea. Journal of Geophysical Research: Oceans, 109(C10). 2004.

O'Dea, S.A., Gibbs, S.J., Bown, P.R., Young, J.R., Poulton, A.J., Newsam, C., Wilson, P.A.: Coccolithophore calcification response to past ocean acidification and climate change. Nature communications, 5. 2014.

Okada, H., Honjo, S.: Distribution of coccolithophores in marginal seas along the western Pacific Ocean and in the Red Sea. Marine Biology, 31(3), 271-285. 1975.

Oviedo, A.M., Langer, G., Ziveri, P.: Effect of phosphorus limitation on coccolith morphology and element ratios in Mediterranean strains of the coccolithophore *Emiliania huxleyi*. Journal of Experimental Marine Biology and Ecology. 459, 105-113. 2014.

Paasche, E.: Roles of nitrogen and phosphorus in coccolith formation in *Emiliania huxleyi* (Prymnesiophyceae). European Journal of Phycology, 33(1), 33-42. 1998.

Paasche, E.: A review of the coccolithophorid *Emiliania huxleyi* (Prymnesiophyceae), with particular reference to growth, coccolith formation, and calcification-photosynthesis interactions. Phycologia, 40(6), 503-529. 2001.

Painter, S.C., Poulton, A.J., Allen, J.T., Pidcock, R., Balch, W.M.: The COPAS'08 expedition to the Patagonian Shelf:

Physical and environmental conditions during the 2008 coccolithophore bloom. Continental Shelf Research, 30(18), 1907-1923. 2010.

Pierrot, D.E., Lewis E, Wallace D.W.R.: MS Excel program developed for CO_2 system calculations. ORNL/CDIAC-105a, Carbon Dioxide Information Analysis Centre, Oak Ridge National Laboratory, US Department of Energy, Oak Ridge, TN. 2006.

Poulton, A.J., Sanders, R., Holligan, P.M., Stinchcombe, M.C., Adey, T.R., Brown, L., Chamberlain, K.: Phytoplankton mineralization in the tropical and subtropical Atlantic Ocean. Global Biogeochemical Cycles, 20(4). 2006.

Poulton, A.J., Adey, T.R., Balch, W.M., Holligan, P.M.: Relating coccolithophore calcification rates to phytoplankton community dynamics: regional differences and implications for carbon export. Deep Sea Research Part II: Topical Studies in Oceanography, 54(5), 538-557. 2007.

Poulton, A. J., Charalampopoulou, A., Young, J.R., Tarran, G.A., Lucas, M.I., Quartly, D.: Coccolithophore dynamics in non‐bloom conditions during late summer in the central Iceland Basin (July‐August 2007). Limnology and Oceanography, 55(4): 1601-1613, 2010.

Poulton, A.J., Young, J.R., Bates, N.R., Balch, W.M.: Biometry of detached *Emiliania huxleyi* coccoliths along the Patagonian Shelf. Marine Ecology Progress Series, 443: 1-17. 2011.

Poulton, A.J., Painter, S.C., Young, J.R., Bates, N.R., Bowler, B., Drapeau, D., Lyczsckowski, E., Balch, W. M.: The 2008 *Emiliania huxleyi* bloom along the Patagonian Shelf: ecology, biogeochemistry, and cellular calcification. Global Biogeochemical Cycles, 27(4), 1023-1033. 2013.

Poulton, A.J., Stinchcombe, M.C., Achterberg, E.P., Bakker, D.E., Dumousseaud, C., Lawson, H.E., Lee, G.A., Richier, S., Suggett, D.J., Young, J. R.: Coccolithophores on the north-west European shelf: calcification rates and environmental controls. Biogeosciences, 11(14), 3919-3940. 2014.

Raitsos, D.E., Lavender, S.J., Pradhan, Y., Tyrrell, T., Reid, P.C., Edwards, M.: Coccolithophore bloom size variation in response to the regional environment of the subarctic North Atlantic. Limnology and Oceanography, 51(5), 2122-2130. 2006.

Riebesell, U., Zondervan, I., Rost, B., Tortell, P.D., Zeebe, R.E., Morel, F.M.M.: Reduced calcification of marine plankton in response to increased atmospheric CO_2. Nature, 407(6802): 364-367. 2000.

Riebesell, U., Tortell, P.D.: Effects of ocean acidification on pelagic organisms and ecosystems. Ocean acidification. Oxford University Press, Oxford, 99-121. 2011.

Rosas-Navarro, A., Langer, G., and Ziveri, P.: Temperature affects the morphology and calcification of *Emiliania huxleyi* strains, Biogeosciences, 13, 2913-2926, doi:10.5194/bg-13-2913-2016, 2016.

Rost, B., Riebessell, U.: Coccolithophores and the biological pump: responses to environmental changes. In Coccolithophores: from molecular processes to global impact. Edited by Thierstein H.R., Young, J.R., Springer-Verlag Berlin Heidelberg. 2004.

Saavedra-Pellitero, M., Baumann, K. H., Flores, J. A., Gersonde, R.: Biogeographic distribution of living coccolithophores in the Pacific sector of the Southern Ocean. Marine Micropaleontology, 109, 1-20. 2014.

Saruwatari, K., Satoh, M., Harada, N., Suzuki, I., Shiraiwa, Y.: Change in coccolith size and morphology due to response to temperature and salinity in coccolithophore *Emiliania huxleyi* (Haptophyta) isolated from the Bering and Chukchi seas. Biogeosciences, 13(9), 2743-2755. 2016.

Satoh, M., Iwamoto, K., Suzuki, I., Shiraiwa, Y.: Cold stress stimulates intracellular calcification by the coccolithophore, *Emiliania huxleyi* (Haptophyceae) under phosphate-deficient conditions. Marine Biotechnology, 11(3), 327-333. 2009.

Schlitzer, R.: Ocean Data View. http://odv.awi.de. 2015.

Shih, Y.Y., Hung, C.C., Gong, G.C., Chung, W.C., Wang, Y.H., Lee, I.H., Chen, K.S., Ho, C.Y.: Enhanced Particulate Organic Carbon Export at Eddy Edges in the Oligotrophic Western North Pacific Ocean. PloS one, 10(7), 2015.

Smith, H. E. K., Tyrrell, T., Charalampopoulou, A., Dumousseaud, C., Legge, O. J., Birchenough, S., Petit, L. R., Garley, R., Herman,M. C., Sagoo, N., Daniels, C. J., Achterberg, E., and Hydes, D. J.: Predominance of heavily calcified coccolithophores at low $CaCO_3$ saturation during winter in the Bay of Biscay, Proceedings of the National Academy of Sciences. 109, 8845–8849, 2012.

Sorrosa, J. M., Satoh, M., Shiraiwa, Y.: Low temperature stimulates cell enlargement and intracellular calcification of coccolithophorids. Marine Biotechnology, 7(2), 128-133, 2005.

Sprengel, C., Baumann, K.H., Neuer, S.: Seasonal and interannual variation of coccolithophore fluxes and species composition in sediment traps north of Gran Canaria (29N 15W). Marine Micropaleontology, 39(1): 157-178. 2000.

Sprengel, C., Baumann, K.H., Henderiks. J., Henrich, R., Neuer, S.: Modern coccolithophore and carbonate sedimentation along a productivity gradient in the Canary Islands region: seasonal export production and surface accumulation rates. Deep Sea Research Part II: Topical Studies in Oceanography, 49(17): 3577-3598. 2002.

Sun, J., An. B. Z., Dai. M. H., Li. T. G.: Living coccolithophores in the western South China Sea in summer 2007, Oceanologia et Limnologia Sinica, 42(2), 170-178. 2011. (in Chinese)

Triantaphyllou, M., Dimiza, M., Krasakopoulou, E., Malinverno, E., Lianou, V., Souvermezoglou, E.: Seasonal variation in *Emiliania huxleyi* coccolith morphology and calcification in the Aegean Sea (Eastern Mediterranean). Geobios, 43(1), 99-110. 2010.

Tseng, C.M., Wong, G.T., Lin, I.I., Wu, C.R., Liu, K.K.: A unique seasonal pattern in phytoplankton biomass in low‐latitude waters in the South China Sea. Geophysical Research Letters, 32(8). 2005.

Wang, G., Su, J., Chu, P.C.: Mesoscale eddies in the South China Sea observed with altimeter data. Geophysical Research Letters, 30(21). 2003.

Wang, L., Huang, B., Chiang, K.P., Liu, X., Chen, B., Xie, Y., Xu, Y., Hu, J., Dai, M.: Physical-Biological Coupling in the Western South China Sea: The Response of Phytoplankton Community to a Mesoscale Cyclonic Eddy. PloS one, 11(4). 2016.

Wang, P., Li, Q., Li, C.F.: Geology of the China Seas. Elsevier. 2014.

Wei, J.W.: Variability in beam attenuation and the suspended particles in the West Philippine Sea. PHD thesis in Chinese Academy of Sciences. 2005. (in Chinese)

Winter, A., Jordan, R.C., Roth, P.H.: Biogeography of living coccolithophores in ocean waters. In Coccolithophores, edited by Winter, A. and Siesser, W.G., Cambridge University Press. 1994.

Wong, G. T., Ku, T. L., Mulholland, M., Tseng, C. M., Wang, D. P.: The South East Asian time-series study (SEATS) and the biogeochemistry of the South China Sea—an overview. Deep Sea Research Part II: Topical Studies in Oceanography, 54(14), 1434-1447. 2007.

Xie, S.P., Xie, Q., Wang, D., Liu, W.T.: Summer upwelling in the South China Sea and its role in regional climate variations. Journal of Geophysical Research: Oceans, 108(C8). 2003.

Xiu, P., Chai, F.: Modeled biogeochemical responses to mesoscale eddies in the South China Sea. Journal of Geophysical Research: Oceans (1978–2012), 116(C10). 2011.

Young, J.R.: Functions of coccoliths. In Coccolithophores, edited by Winter, A. and Siesser, W.G., Cambridge University Press. 1994.

Young, J.R., Ziveri, P.: Calculation of coccolith volume and it use in calibration of carbonate flux estimates. Deep sea research Part II: Topical studies in oceanography, 47(9): 1679-1700. 2000.

Young, J.R., Geisen, M., Cros, L., Kleijne, A., Sprengel, C., Probert, I., Østergaard, J.: A guide to extant coccolithophore taxonomy. International Nannoplankton Association. 2003.

Young, J.R., Poulton, A.J., Tyrrell,T.: Morphology of *Emiliania huxleyi* coccoliths on the northwestern European shelf - Is there an influence of carbonate chemistry?. Biogeosciences, 11(17). 4771-4782. 2014.

Zhou, K.B., Dai, M.H., Kao, S.J., Wang, L., Xiu, P., Chai, F., Tian, J.W., Liu, Yang.: Apparent enhancement of ^{234}Th-based particle export associated with anticyclonic eddies. Earth and Planetary Science Letters, 381: 198-209. 2013.

Ziveri, P., de Bernardi, B., Baumann, K.H., Stoll, H.M., Mortyn, P.G.: Sinking of coccolith carbonate and potential contribution to organic carbon ballasting in the deep ocean. Deep Sea Research Part II: Topical Studies in Oceanography, 54(5), 659-675. 2007.

Tables

Table 1. Sampling date, location, depth and upper water structure conditions: mixed layer depth (MLD), euphotic zone depth (Zeu).

Station	Date (GMT+8)	Longitude	Latitude	Sampling depth (m)	MLD (m)	Zeu (m)
D9	2014/6/25 7:11	119	18	25,50,75,100,150	34	95
F1	2014/6/26 3:38	118	18	25,50,75,100,150	24	92
G2	2014/6/26 14:36	117	18	25,45,75,100,150	12	90
H3	2014/6/27 15:08	116	18	25,60,75,100,150	11	98
I1	2014/6/20 0:52	115	19.5	25,50,100	16	76
I2	2014/6/20 20:50	115	19	25,50,75,100,150	16	69
I3	2014/6/29 9:23	115	18	25,50,75,100,150	23	99
J1	2014/6/29 20:35	114	18	25,50,75,100,150	26	98
X3	2014/6/30 6:58	113	18	25,50,75,100,150	30	100
X4	2014/6/30 18:01	112	18	25,50,75,100,150	35	99
X5	2014/7/1 5:10	111	18	25,50,75,100,150	17	93
I4	2014/7/9 8:23	115	17	25,50,75,100,150	18	
I5	2014/7/9 1:54	115	16	25,50,75,100,150	(<25)	
I6	2014/7/8 17:53	115	15	25,50,75,100	(>25)	
I7	2014/7/7 22:33	114.67	14	25,50,75,100,150	20	

Table 2. Coccolithophore species composition in Group 1, Group 2 and Group 3. R: mean relative abundance; F: occurrence frequency. Bold numbers indicate the representative species in their groups.

	Group 1		Group 2		Group 3	
	R	F	R	F	R	F
Algirosphaera robusta	0.39	23.53	2.22	66.67	**19.78**	**92.86**
Florisphaera profunda	0.35	17.65	1.34	41.67	**43.81**	**100.00**
Gladiolithus flabellatus	0.00	0.00	0.00	0.00	**1.66**	**60.71**
Emiliania huxleyi	**36.97**	**94.12**	**66.84**	**100.00**	**22.65**	**92.86**
Gephyrocapsa oceanica	2.29	41.18	**10.23**	**91.67**	1.65	46.43
Gephyrocapsa ericsonii	6.20	52.94	6.20	50.00	2.61	32.14
Umbellosphaera irregularis	**34.35**	**94.12**	0.86	41.67	0.24	7.14
Umbellosphaera tenuis	2.14	47.06	0.10	16.67	0.00	0.00
Discosphaera tubifera	**4.41**	**82.35**	0.11	8.33	0.00	0.00
Rhabdosphaera clavigera	0.82	23.53	0.04	8.33	0.00	0.00
Calcidiscus leptoporus	0.82	17.65	1.53	58.33	0.96	35.71
Oolithotus fragilis	3.64	35.29	**6.95**	**83.33**	**3.87**	**78.57**
Helicosphaera carteri	1.05	58.82	0.21	25.00	0.03	3.57
Syracosphaera spp.	3.92	94.12	1.56	83.33	1.55	53.57
Umbilicosphaera sibogae	0.45	17.65	0.71	33.33	0.22	14.29
Calciosolenia spp.	0.49	23.53	0.48	58.33	0.41	21.43
Michaelsarsia spp.	1.71	35.29	0.61	41.67	0.54	25.00

Table 3. Pearson's product-moment correlations (r) between mean distal shield length (DSL) of *E. huxleyi*, principal component-1 (PC-1) scores and environmental parameters: nitrate+nitrite (N), phosphate (P), pH, total alkalinity (A_T), $CaCO_3$ saturation (Ω_C), temperature (T) (n=29). The principal component analysis is based on all the environmental parameters, with PC-1 contrition 76.59% to total variance. ***** $p<0.05$; ****** $p<0.01$.

	mean DSL	PC-1 (76.59%)
N	0.601**	-0.967**
P	0.579**	-0.965**
pH	-0.526**	0.804**
A_T	0.274	-0.671**
Ω_C	-0.395*	0.958**
T	-0.21	0.842**

Figure 1:

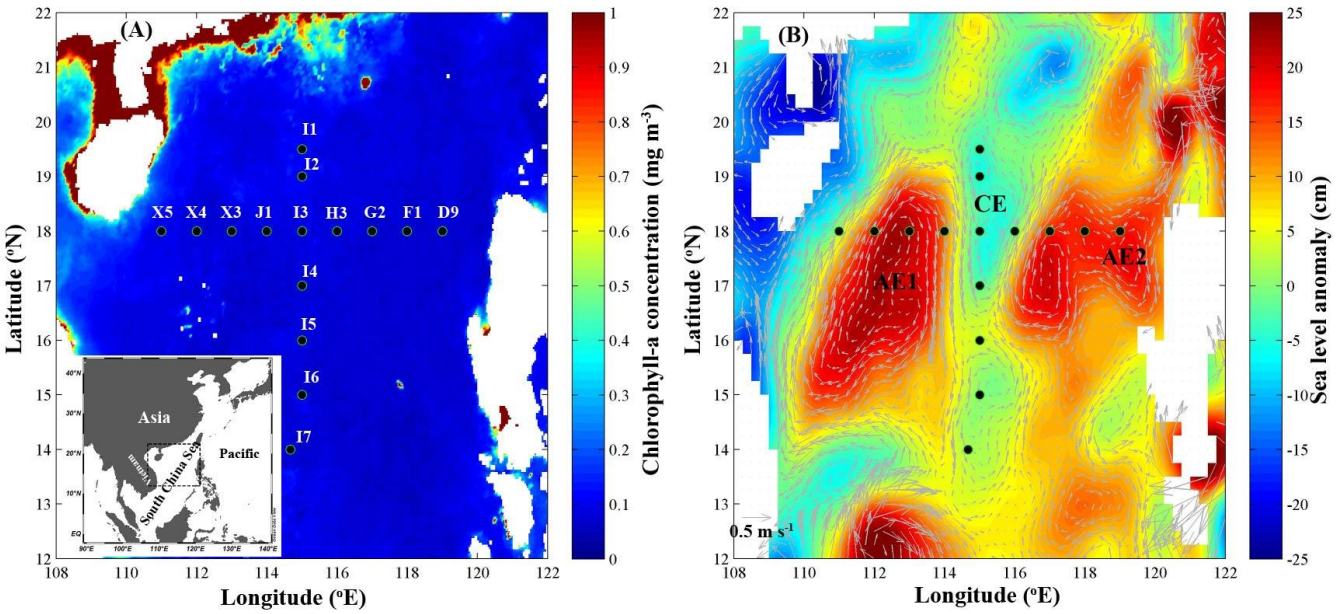

Figure 1: (A) Sampling stations in the SCS, superimposed on the MODIS-Aqua (4 km) monthly average (May to August 2014) surface chlorophyll-*a* (mg m^{-3}). (B) Map of sea level anomaly (SLA) and geostrophic flow in 30th June 2014. The positive SLA with clockwise flow indicates anti-cyclonic eddies (AE), and the negative SLA with anticlockwise flow indicates cyclonic eddies (CE).

Figure 2:

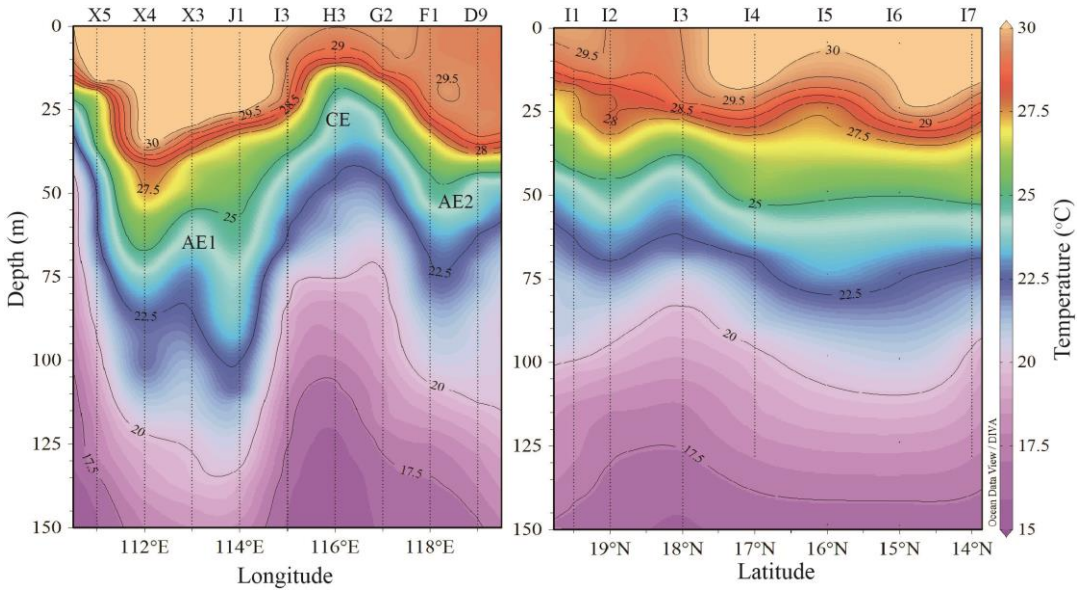

Figure 2: Temperature (℃) profiles in zonal (a) and meridional (b) sections. Variation of isotherm indicates anti-cyclonic eddies (AE) and cyclonic eddy (CE) respectively. Profiles are dawn with Ocean Data View software (Schlitzer, 2015).

Figure 3:

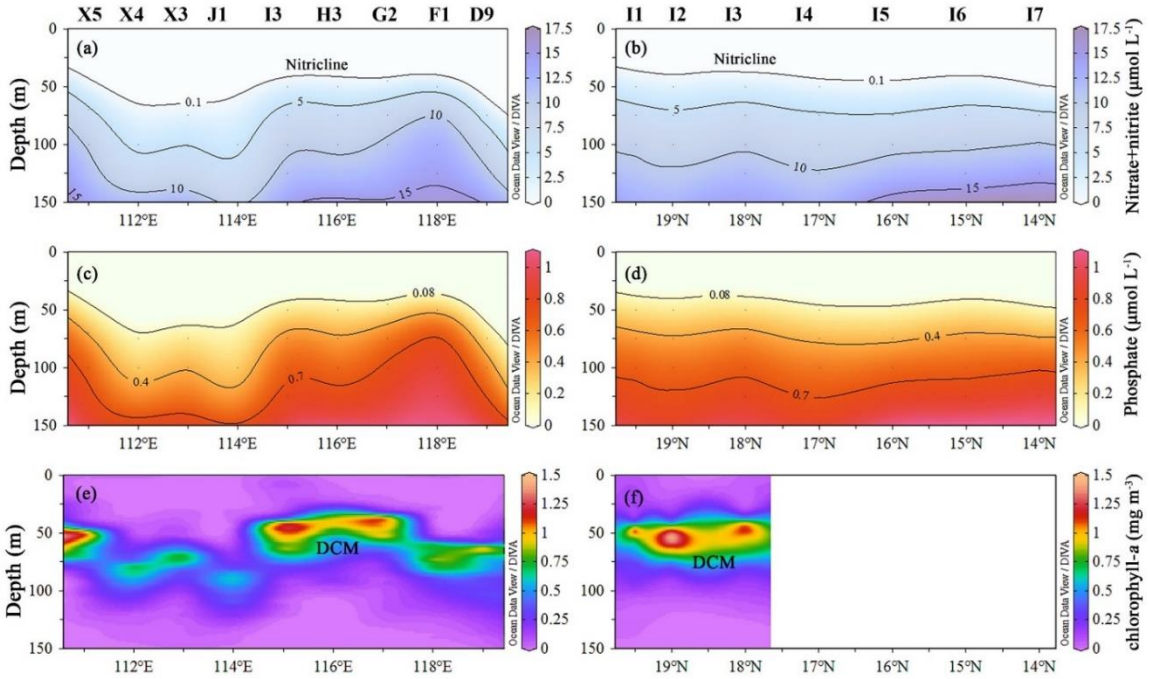

Figure 3: Profiles of macronutrient (nitrate+nitrite, phosphate) condition and chlorophyll-*a* concentration (mg m^{-3}) in zonal (a, c, e) and meridional sections (b, d, f). Nitricline is the depth where nitrate+nitrite is 0.1 µmol L^{-1} (Borgne et al., 2002). DCM: deep chlorophyll-*a* maximum.

Figure 4:

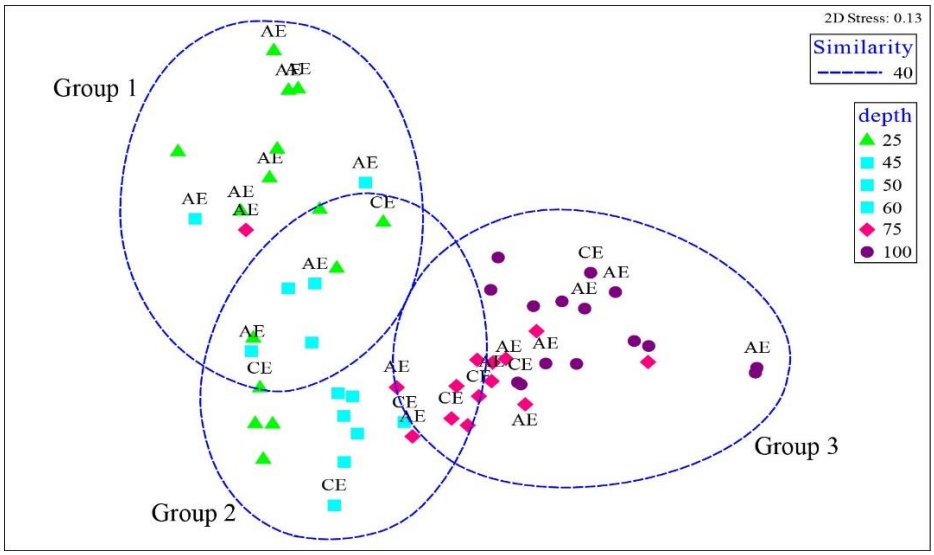

Figure 4: Non-metric Multi-Dimensional Scaling (nMDS) ordination of stations in different depth, based on Bray-Curtis similarity. The stress 0.13 of 2-dimentional ordination can provide a good interpretation for community group (Clarke and Warwick, 2001). The blue dashed lines indicate different divisions at 40 similarity, which is conducted by cluster analysis, using the same resemblance as nMDS. CE: cyclonic eddy; AE: anti-cyclonic eddy.

Figure 5:

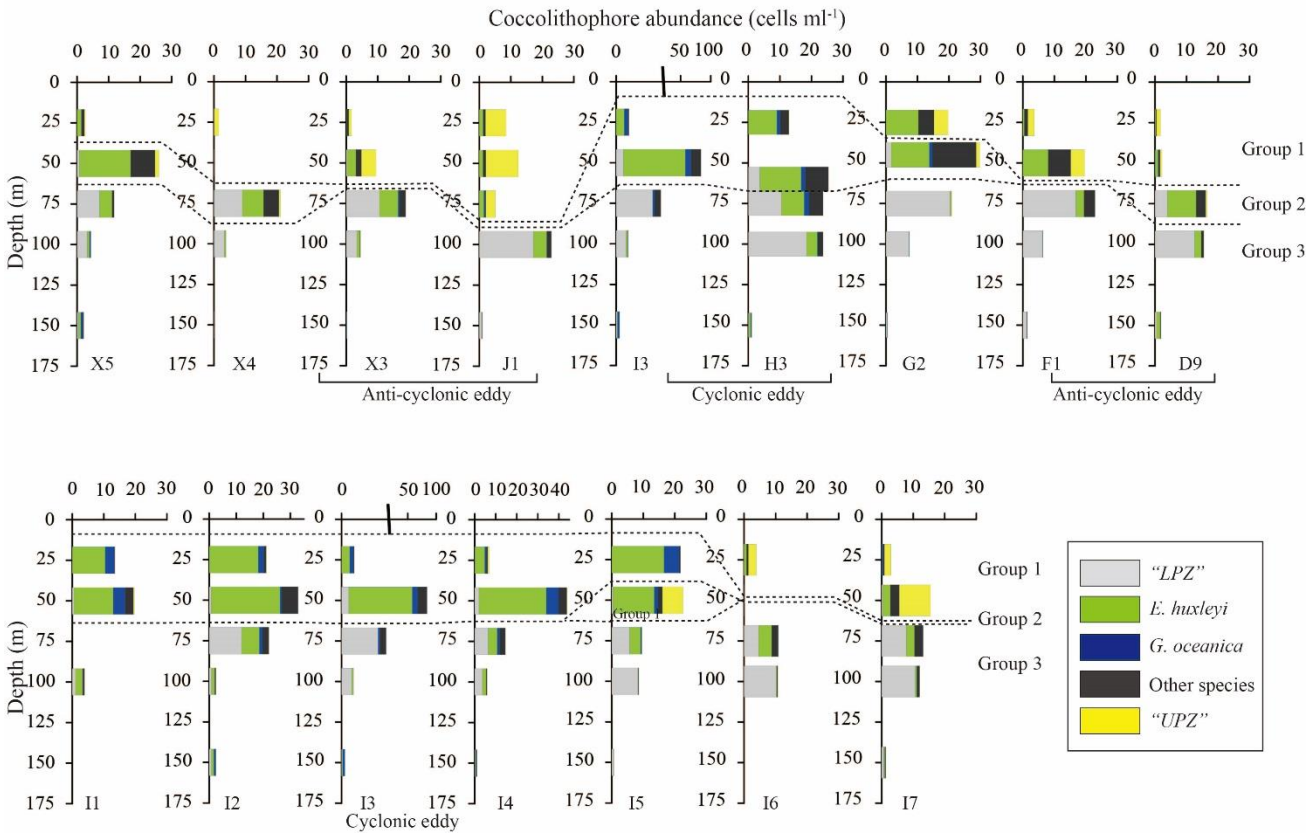

Figure 5: Coccolithophore abundance (cells ml^{-1}) of three groups in sampling stations. "LPZ" specifically indicates three species: *F. profunda, A. robusta* and *G. flabellatus*. "UPZ" specifically indicates: *Umbellosphaera* spp., *D. tubifera* and *R. clavigera*.

Figure 6:

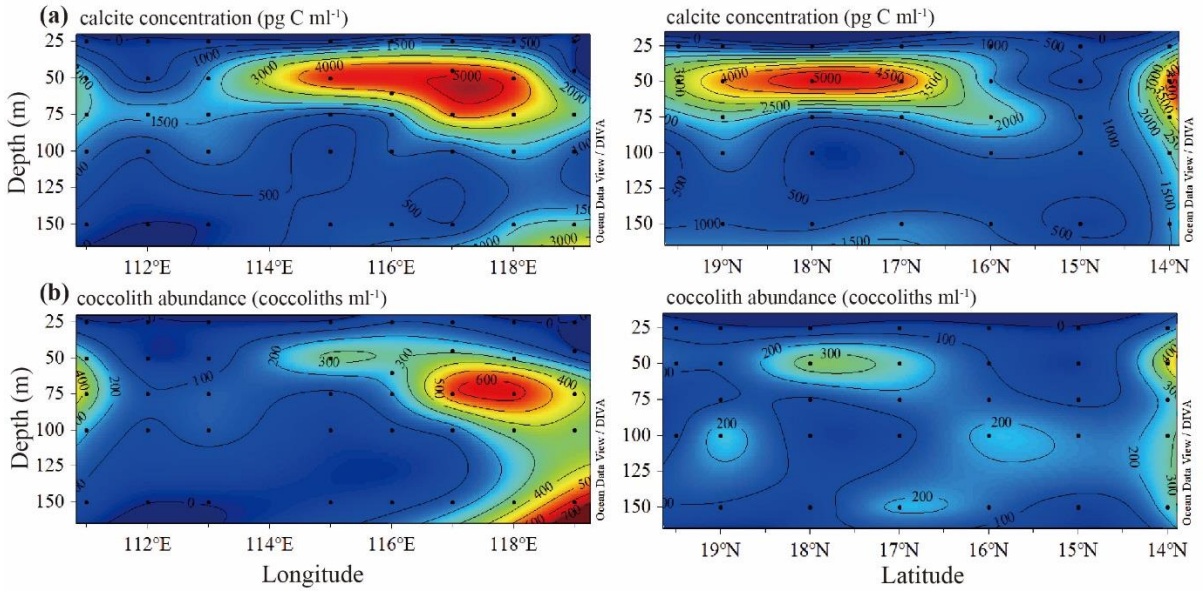

Figure 6: Coccolithophore-based calcite concentration (a) and detached coccolith concentration (b) in zonal and meridional sections.

5

Figure 7:

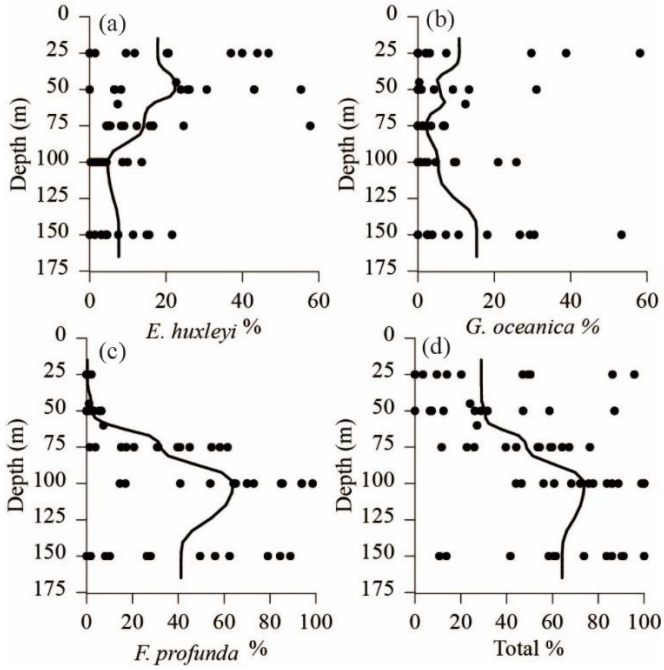

Figure 7: The relative contribution of *E. huxleyi* (a), *F. profunda* (b), *G. oceanica* (c) and their total contribution (d) to coccolithophore-based calcite concentration in water column. The black lines denote moving average of 30 grid-points.

Figure 8:

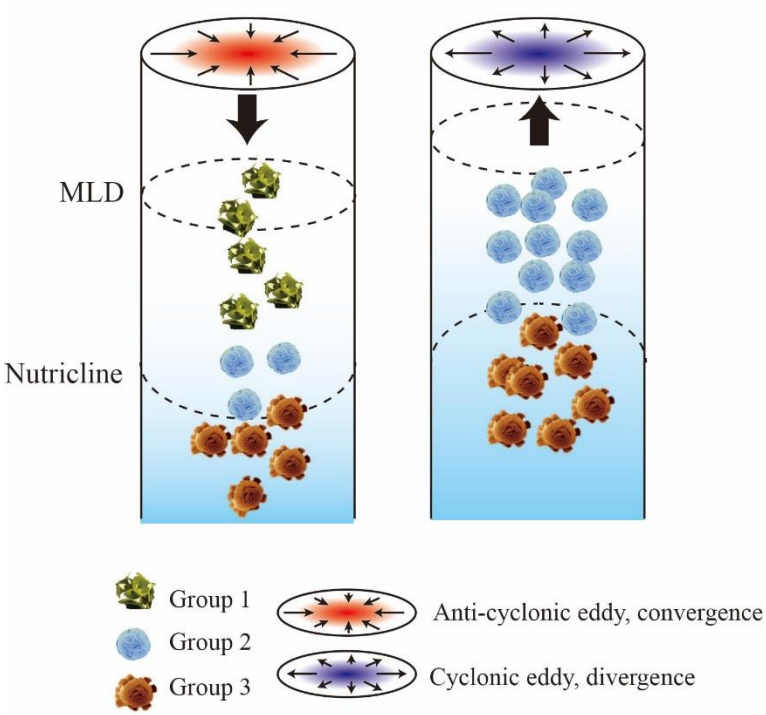

Figure 8: Schematic showing the coccolithophore communities in anti-cyclonic eddy and cyclonic eddy.

5

Figure 9:

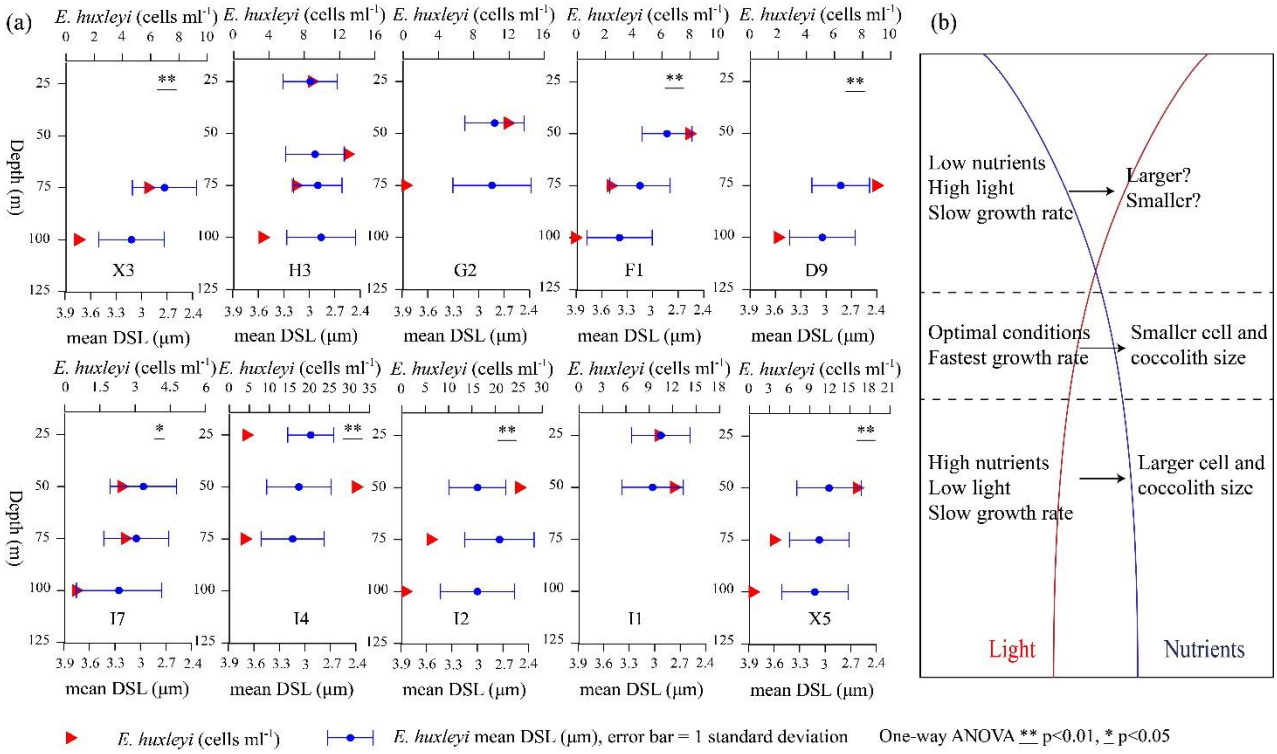

Figure 9: (a) Cell abundance (red triangles) and mean distal shield length (DSL, blue dots, error bar =1 standard deviation) of *E. huxleyi* plotted in stations where there were at least two biometry measurement points. (b) A schematic map showing light and nutrients conditions in relation to coccolithophore growth rate and cell/coccolith size.

Figure 10:

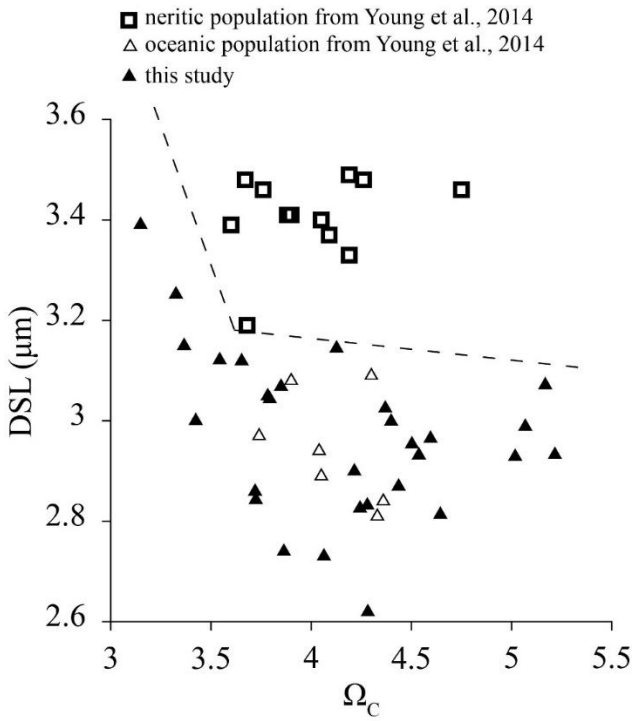

Figure 10: *E. huxleyi* type A distal shield length (DSL) in the SCS (black triangles) with those in neritic (hollow triangles) and oceanic (hollow squares) in the North Sea (Young et al., 2014) plotted versus carbonate calcium saturation (Ω_C).